Westward Propagation of Latitudinal Asymmetry in a Coupled Ocean–Atmosphere Model

SHANG-PING XIE

Graduate School of Environmental Earth Science, Hokkaido University, Japan

(Manuscript received 11 September 1995, in final form 20 March 1996)

ABSTRACT

Hemispheric asymmetries of continental geometry have long been speculated to be the cause of the Northern Hemisphere position of the intertropical convergence zone over the central and eastern Pacific. It is unknown, however, how the effects of continental asymmetries are transmitted to and felt by the central Pacific thousands of kilometers away. This paper proposes a transmitter mechanism by investigating the response of a coupled ocean–atmosphere model to a symmetry-breaking force by the American continents. The model treats land forcing implicitly as an eastern boundary condition. In the absence of oceanic feedback, the model response to the eastern boundary forcing is tightly trapped and confined to a small longitudinal extent off the coast, whereas the climate over the interior ocean is symmetric about the equator. Ocean–atmosphere coupling greatly enhances the transmissibility of the effects of the land forcing, establishing large latitudinal asymmetry over a great zonal extent. A westward propagating coupled instability is found to be responsible, which is antisymmetric about the equator and is caused by a wind–evaporation–SST feedback proposed previously by Xie and Philander. The solution to an initial value problem shows that a coupled ocean–atmosphere wave front generated by the land forcing amplifies as it moves westward, leaving behind a latitudinally asymmetric steady state.

1. Introduction

The intertropical convergence zone (ITCZ), characterized by heavy rainfall, high cloudiness and surface wind convergence, is the ascending branch of the global Hadley circulation. It has been known for a long time that over a large zonal extent covering the central and eastern Pacific, the ITCZ is located in the Northern Hemisphere (NH) instead of being centered on the equator as one may expect from the meridional distribution of solar radiation (Kornfield et al. 1967). The cause of the Pacific ITCZ's departure from the equator is the focus of this study.

Both the annual mean position and the seasonal movement of the ITCZ display large variation in the zonal direction. Over continents, the ITCZ moves north- and southward across the equator during a year, following the seasonal march of the sun. Similar cross-equatorial movement of the ITCZ is seen over the warm water pool region in the Indian and western Pacific Oceans, where, with little difference in sea surface temperature (SST) across the equator, solar radiation is the determining factor for the location of the ITCZ. In the other oceanic sectors of the equatorial belt, namely over the Atlantic and the central and eastern Pacific, the ITCZ persists in the Northern Hemisphere (Mitchell and Wallace 1992). Equatorial asymmetry in the SST distribution, with higher SSTs to the north than to the south of the equator, is responsible for the Northern Hemisphere position of the ITCZ in these regions. In March and April, when latitudinal asymmetry in SST is minimal, a symmetric double ITCZ appears in the eastern Pacific. Experiments with atmospheric general circulation models (AGCM) confirm the importance of SST in determining the configuration of the ITCZ (Manabe et al. 1974). Therefore, to completely solve the ITCZ problem one should ask not only why the ITCZ stays in the Northern Hemisphere, but also why the SST is high to the north of the equator. As for the latter question, oceanographic studies suggest that among many effects of wind forcing, the latitudinal asymmetry in scalar wind speed contributes the most to the observed asymmetric distribution of the SST through surface latent heat flux (Xie 1994a).

The essential involvement of the ocean calls for an approach of ocean–atmosphere coupling to the problem. In a coupled ocean–atmosphere model under equatorially symmetric conditions, Xie and Philander (1994) found self-sustaining asymmetric steady states with a single ITCZ forming only in one hemisphere. A positive wind–evaporation–SST (WES) feedback, internal to the ocean–atmosphere system, breaks the equatorial symmetry set by solar radiation, leading the tropical climate to a latitudinally asymmetric state (Xie

Corresponding author address: Dr. Shang-Ping Xie, Graduate School of Environmental Earth Science, Hokkaido University, Sapporo 060, Japan.
E-mail: xie@eoas.hokudai.ac.jp

1996a).[1] While suggesting that the ocean–atmosphere system prefers latitudinally asymmetric states, the above studies do not answer the question of why the Northern Hemisphere is favored on the earth. It seems that the Northern Hemisphere mode is selected on the earth not by chance. If so, we should have a chance to see the ITCZ persist in the Southern Hemisphere after a major El Niño event, during which the SST and precipitation are nearly symmetric about the equator.

Hemispheric asymmetries in such geographic features of the earth's continents as landmass, topography, and coastal line orientation have long been speculated, but never demonstrated, to be the cause of the NH position of the Pacific ITCZ. A counter-example against these hypotheses of geographical determination exists in the Indian Ocean, however. Annual-mean precipitation and SST are nearly symmetric about the equator in the Indian Ocean,[2] where the largest hemispheric asymmetry in the landmass distribution occurs and whose eastern boundary, Sumatra Island, slants northwestward, an orientation favoring a Northern Hemisphere ITCZ. While indicating that geographic asymmetry is not the sufficient condition for a NH ITCZ, the above example of the Indian Ocean does not rule out the possibility that it serves as a mode selector for the coupled ocean–atmosphere. The proof of this possibility requires an answer to the question of how the central and eastern Pacific feels the influences of geographic asymmetries thousands of kilometers away on the American continents. The atmosphere itself is not a good transmitter of land forcing, however. The atmospheric response to continental asymmetries in the Americas is damped rapidly toward the west, and trapped and confined to a small zonal extent off the coast, as demonstrated by Philander et al. (1996, manuscript submitted to *J. Climate*) with an idealized AGCM that removes zonal and hemispheric asymmetries in SST. An efficient transmitter that involves both the atmosphere and the ocean is, thus, necessary to explain the large zonal scale of the observed Pacific NH ITCZ.

This paper explores and examines ocean–atmosphere interactions that transmit the signals of land geographic asymmetry into the deep interior Pacific to the west. Xie and Philander's (1994) coupled model, which consists of a Matsuno–Gill atmosphere and a mixed layer ocean forced by heat fluxes, will be used and extended to allow zonal variations. The land–atmospheric interactions are not treated explicitly, but are implicitly included by imposing their effects on the atmospheric circulation as the eastern boundary conditions of the ocean–atmosphere model. This implicit treatment of land effects enables us to focus on the interaction between the ocean and atmosphere and allows a smooth connection to existing theories. This investigation of ocean–atmospheric response to land forcing could serve as a stepping stone toward understanding the more complicated problem of three-component interaction of the ocean, atmosphere, and land. Westward propagating ocean–atmosphere waves, which are antisymmetric about the equator and different from the equatorially symmetric El Niño–Southern Oscillation (ENSO) modes of Hirst [1986; see Neelin et al. (1994) for a review], exist in the model, providing the mechanism that bridges the land and the interior ocean to the west. The WES feedback is the restoring force for these ocean–atmosphere waves. Because of these westward propagating waves, the symmetry-breaking force of land is transmitted toward the west, establishing a NH ITCZ over a great zonal extent as is observed in the Pacific.

The next section describes the numerical experiments with the extended Xie and Philander model. Section 3 derives the low-order model, and section 4 gives its steady-state solution. Section 5 solves time-dependent problems and examines the roles of coupled WES waves in the ocean–atmospheric adjustment toward a steady state, a problem similar to the transient spinup problem of Anderson and Gill (1975). Section 6 presents the results when nonlinear effects are important and discusses the application of this theory to the real Pacific. Section 7 is the summary.

2. Numerical experiments

a. Model

The shallow water equations model of Matsuno (1966) and Gill (1980) is adopted for the atmosphere:

$$\epsilon U - YV = -\Phi_X, \tag{2.1}$$

$$\epsilon V + YU = -\Phi_Y, \tag{2.2}$$

$$\epsilon\Phi + U_X + V_Y = -Q, \tag{2.3}$$

where U and V are the zonal and meridional low-level wind velocities, Φ is the geopotential, (X, Y) are the zonal and meridional coordinates nondimensionalized with the equatorial radius of deformation, and $\epsilon = A/(\beta C)^{1/2}$ is the nondimensional damping rate with A its dimensional counterpart, β the meridional gradient of the Coriolis parameter, and C the phase speed of the long gravity wave. Advection by mean winds is not considered here since tropical wind speed is generally much smaller than the long gravity wave speed $C = 45$ m s^{-1}.

[1] A similar feedback is found to be at work in a state-of-the-art coupled GCM (Robertson et al. 1995).

[2] The observed SST distribution is asymmetric about the equator at all longitudes in an exact sense. One may, however, define the equatorial symmetry in a less strict way, for example, by measuring the departure from the equator of the center of mass of a meridional SST profile at a longitude. The size of the surface meridional wind at the equator is a good index of equatorial asymmetry, as will be seen in the next section.

Latent heat release to the atmosphere by precipitating convection is parameterized as a function of SST with a threshold $T_c = 27.5°C$,

$$Q = \frac{K_Q}{(\beta C^3)^{1/2}}(T - T_c)H(T - T_c), \quad (2.4)$$

where $H(x)$ is the Heaviside function. Geographical correspondence between the areas of high SST and of active convection is apparent in the Tropics. Deep convection preferentially occurs over warm sea surface because high SSTs permit large moisture contents near the surface and reduce the moist static stability of the lower atmosphere. Equation (2.4) has been used in coupled ocean–atmosphere models of ENSO (Anderson and McCreary 1985; Xie et al. 1989) and of the ITCZ (Xie and Philander 1994). This study focuses on the eastern Pacific, where the SST distribution is characterized by a minimum near the equator. The empirical relation (2.4) seems to work well in the eastern Pacific, as manifested by the in-phase seasonal variations in SST and in the intensity of the Pacific NH ITCZ. In the western Pacific, on the other hand, the warm pool has a broad meridional extent and factors other than SST seem to play a role as well in positioning the ITCZ. In AGCMs forced by such a western Pacific-type SST distribution, the configuration of the ITCZ is sensitive to convective parameterization (Numaguti and Hayashi 1991; Hess et al. 1993).

The ocean contains a mixed layer of a constant depth h whose temperature T is determined by the equation

$$\frac{\partial T}{\partial t} = \frac{Q_0 - Q_w - C_E^* |\mathbf{U}| q(T)}{\rho c_p h} + \kappa \nabla^2 T, \quad (2.5)$$

where ρ and c_p are the density and specific heat of water, κ is the diffusivity and Q_0 is the radiative flux including both the solar and longwave radiation. The term Q_w represents the effect of advection by ocean currents. Upwelling/downwelling is an important mechanism for SST changes near the equator (Hirst 1986; Neelin and Dijkstra 1995). At the latitudes of the NH warm SST band that is a few oceanic radii of deformation off the equator, however, geostrophy prevails and vertical motion is suppressed. Xie (1994a) shows that in an OGCM, nearly all the SST difference between 10°N and 10°S is attributable to the difference in scalar wind speed (Xie's Fig. 5a). In this study the cooling by equatorial upwelling and poleward advection Q_w is prescribed as a function of latitude that peaks at and is symmetric about the equator. The prescribed cooling prevents the ITCZ from forming on the equator, a situation characterizing the eastern Pacific. The absence of active ocean dynamics in the model suppresses the ENSO modes, allowing us to focus on processes that break the equatorial symmetry. A hybrid coupled OGCM with explicit ocean dynamics gives qualitatively the same results as the present simple model (not shown).

The third term in (2.5) is surface latent heat flux, with C_E^* being the evaporation coefficient and q the saturated moisture content given by the Clausius–Clapeyron equation. In the steady state, and if diffusion is small, the latent heat flux, a function of both wind speed $|\mathbf{U}|$ and SST, balances the radiative flux plus dynamic cooling, thus being symmetric about the equator (Fig. 4a). A latitudinally asymmetric wind field therefore leads to latitudinal asymmetry in SST. In a transient sense, on the other hand, a decrease in wind speed reduces latent heat flux, leading to a increase in local SST. This is the essential ingredient of the WES feedback.

Equations (2.1)–(2.5) form our coupled ocean–atmosphere model, where the atmosphere forces the ocean by modifying latent heat flux. A constant background wind, $U_0 = -4$ m s^{-1}, is imposed to mimic the tropical easterly winds maintained by eddy momentum transport in the zonally symmetric circulation. Thus, the zonal wind used to force the ocean is

$$U^* = U_0 + U. \quad (2.6)$$

The model results are not qualitatively sensitive to the size of U_0. A minimum wind speed of 4 m s^{-1} is used for evaporation calculation if the model wind speed falls below this value, mimicking the effects of high-frequency atmospheric disturbances. The diffusion of temperature in the zonal direction is negligible compared to that in the meridional direction, because of the small ratio of the meridional to the zonal scale. As a result, the SST at one longitude is essentially independent of that at the other. The response of the atmospheric model to a zonally asymmetric forcing is nonlocal, however, consisting of both locally and remotely forced components with the latter taking the form of damped equatorial waves. In a zonally uniform setting, an equatorially antisymmetric instability mode exists in the coupled model (Xie 1996a).

A single tropical ocean basin is considered, with dimensions of $-12\,800$ km $\leq x \leq 0$ and $|y| \leq 3000$ km. The atmosphere is cyclic in the zonal direction with a dimension of $-25\,600$ km $\leq x \leq 0$. Area outside the oceanic domain may be considered to be land surface, where the heating to the atmosphere is set to zero. The poleward boundaries of the atmosphere are located at $y = \pm 4500$ km, where the condition of vanishing meridional velocity is imposed. The zero lateral flux condition is imposed on the boundaries of the ocean. The ocean model is solved by the finite difference method and the atmosphere by the semispectral method that applies the Fourier expansion in the zonal direction. All the variables share the same grid points with the size of the grids being 400 km in the zonal and 100 km in the meridional direction. External parameters and functions are the same as Xie and Philander (1994), with $A = (2 \text{ days})^{-1}$, $h = 50$ m, and $\kappa = 2 \times 10^3$ m^2 s^{-1} to list a few. A smaller thermal coupling coefficient, $K_Q = K_Q^0 = 2.4 \times 10^{-3}$ m^2 s^{-3} K^{-1}, is used

here. The dependence on K_Q will be examined in section 4.

b. *Numerical solutions*

With the above selection of parameters, the WES mode is unstable and calculations confirm that equatorially asymmetric solutions exist in a meridionally one-dimensional version of the model that assumes zonal uniformity. Such a zonally symmetric solution is not possible, however, in a model configuration with a larger atmospheric domain because of the land–sea contrast. The only solution to the two-dimensional model, independent of initial conditions, is symmetric about the equator as displayed in Fig. 1. As will be seen in the next few sections, the symmetrization is due to the latitudinal symmetric condition over land that requires convective heating to vanish. The symmetric solution has a double ITCZ structure at all longitudes. The SST is cold at the equator and increases away from it, a manifestation of the imposed equatorial upwelling cooling. The land–sea contrast in heating weakens the winds in the western ocean, leading to high SSTs. In the east there is a cold tongue, forming a zonal contrast in SST. The zonal SST variation is a result of its interaction with the winds, as discussed by Neelin and Dijkstra (1995) in a different model context. In the eastern ocean the model SST is too cold, and the zonal winds are too strong in the model compared to observations, presumably due to the lack of the blocking of zonal winds by the Andes. This defect has little effects on other model features, however, since the equatorial SST is below the threshold for convection.

The symmetrization of the ITCZ by the addition of the zonal dimension is consistent with the results of Philander et al. (1996, manuscript submitted to *J. Climate*) and Li and Philander (1996). These results suggest that asymmetries external to the Pacific ocean–atmosphere system are necessary for the observed NH ITCZ. A simple model such as the present one is obviously not suitable to treat the land processes directly. If we can characterize the effects of these land processes, however, it is still possible within the present model framework to investigate how these land effects

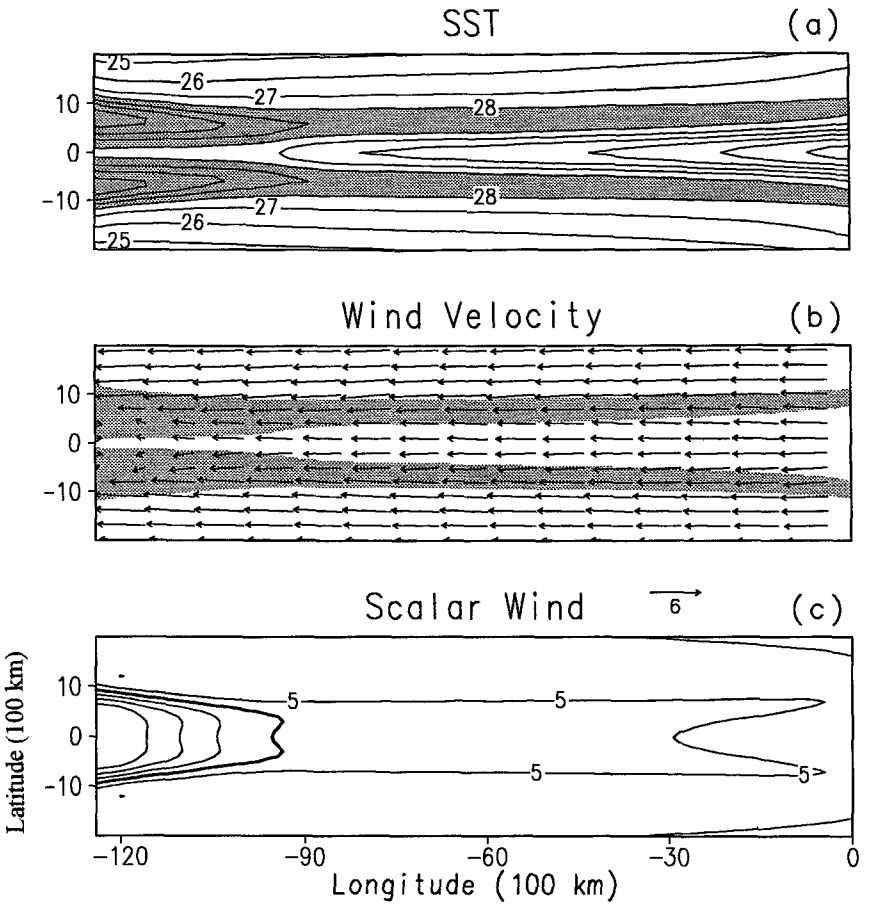

FIG. 1. Horizontal distributions of (a) SST (°C), (b) surface wind velocity, and (c) scalar wind speed (m s^{-1}). SST > 28°C is shaded.

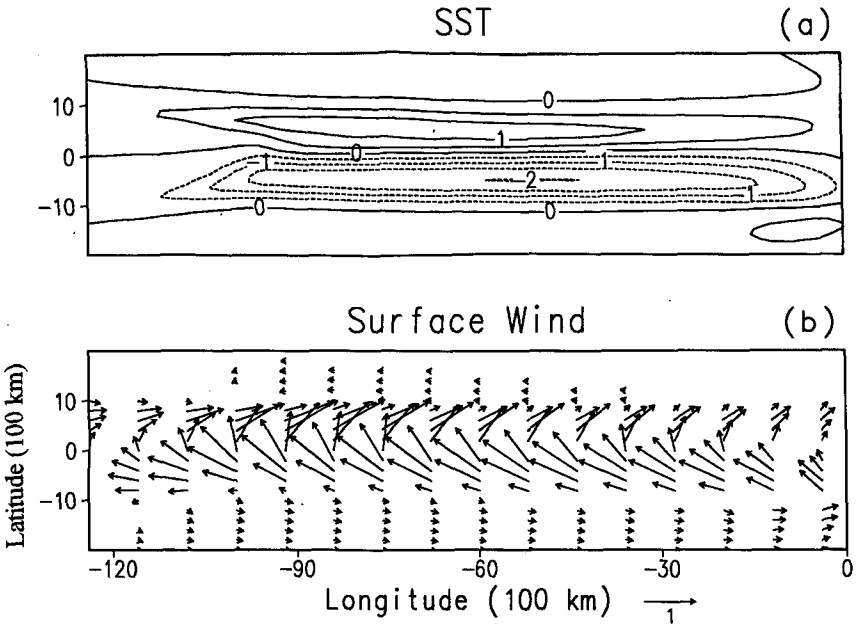

FIG. 2. Land-forced departures from the symmetric solution shown in Fig. 1: (a) sea surface temperature (negative in dashed lines) and (b) wind velocity.

influence the Pacific ocean–atmosphere system. In fact such an approach with a simple model is desirable at this stage as our understanding of the three-component interaction of the ocean, atmosphere, and land is limited at best. In this paper we limit our scope to the problem of the response of the ocean–atmospheric subsystem to parameterized land forcing. The following is a nonexhaustive list of land features that are often hypothesized as the determinant(s) for the Pacific NH ITCZ.

(i) The southeast–northwest slant of the eastern boundary against a meridian. With such a tilted coast, prevalent easterly trades induce more coastal upwelling to the south than to the north of the equator.

(ii) The topography on the American continents. In contrast to relatively low topography in Central America, the tall mountains of the Andes cause large-scale upward motion to the east and downward motion to the west, in the prevailing easterlies. The topographically forced downward motion, together with the downdraft associated with the South American convection, could suppress convection in the southeast equatorial Pacific.

(iii) The Atlantic NH ITCZ. Its own cause may be attributed to the bulge of the African continent to the north of the equator, as suggested by Philander et al. (1996, manuscript submitted to *J. Climate*).

(iv) Seasonal forcing. Recent CGCM experiments suggest that the seasonal solar forcing is rather a symmetry restoring force, with latitudinal asymmetry of the Pacific ITCZ being much weaker in the seasonal run (Mechoso et al. 1995) than in a permanent equinox run (Philander et al. 1996). In the present simple model, latitudinal asymmetry decreases as the amplitude of seasonal solar forcing increases (Xie 1996b).

A common consequence of hypothesized land effects (i) and (ii) is suppressed convection to the south of the equator. As a crude representation of land effects of (i) and (ii) in this simple ocean–atmosphere model, the heating to the atmosphere is suppressed south of the equator at the easternmost five grid points covering a zonal extent of 2000 km. Upon imposing this asymmetric "land" effect, transient westward propagating features develop (see Figs. 8a and 9). The transient aspects of the problem will be treated in section 5. Figure 2 shows the departures of the land-forced steady-state solution from that under symmetric conditions. The SST is 3°C higher to the north than that to the south of the equator. Inducing southerlies near the equator, such equatorial asymmetries in SST are in turn maintained by asymmetries in trade winds, suggesting that the WES feedback is at work. Figure 3 shows the total fields of the steady-state solution, which are symmetric in the west and asymmetric in the rest of the domain, a feature observed in the Pacific. In the eastern two-thirds of the domain, there is only one major convective zone located in the Northern Hemisphere. The warm SST band supporting the NH ITCZ coincides with the zone of weak easterly trades (Fig. 3b). Compared to observations, meridional winds are too weak because the mechanical damping rate is the same throughout the troposphere in the model. Figure 4 contrasts the

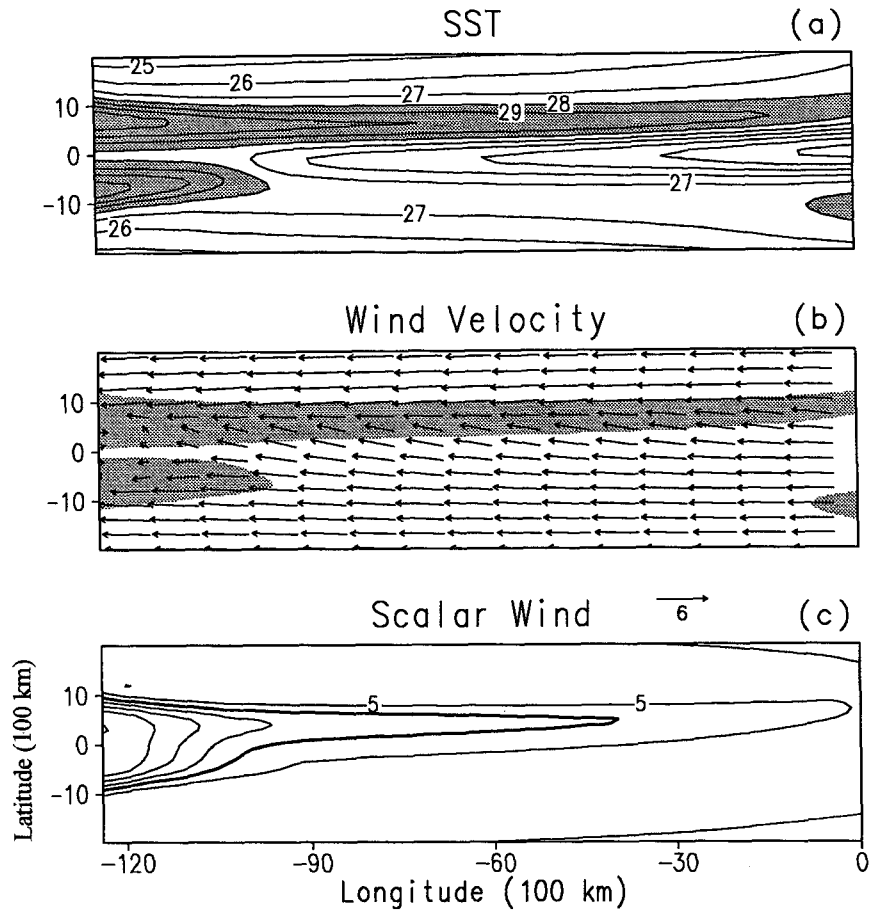

FIG. 3. Same as Fig. 1 except for the land-forced solution.

symmetric and land-forced asymmetric solutions at the middle of the basin. In contrast to the large changes in SST, the difference in latent heat flux between the two solutions is rather small. The latent heat flux remains nearly unchanged from one steady state to the other because it has to balance the same solar radiation distribution as the diffusion is small. In fact, the latent heat flux curves in Fig. 4a are close to the prescribed profile of $Q_0 - Q_w$. The ocean–atmospheric interaction allows the wind speed and SST to adjust and give an amount of latent heat flux that is determined by $Q_0 - Q_w$.

In Fig. 3, there is an area of relatively high SST to the south of the equator near the eastern boundary, an unrealistic feature arising from the crude representation of land forcing. This small pool of warm SST in the southeastern corner, however, falls within the decoupled region not affecting the atmosphere. The western equatorial ocean is also decoupled from the atmosphere because the winds are weak and below the minimum wind speed for evaporation. As a result, both the SST and wind fields are nearly equatorially symmetric.

The ad hoc representation of land forcing here is equivalent to placing a heat sink to the atmosphere in the southeastern corner of the ocean. Without oceanic feedback, this localized heat sink can affect only a limited zonal extent to the west (as illustrated by the response pattern of the atmosphere in Fig. 9a). In contrast, a basinwide response is generated in the coupled ocean–atmosphere model, with equatorially asymmetric anomalies extending all the way to the western boundary (Fig. 2). The rest of the paper attempts to understand how the conditions in the east are transmitted to and felt by the interior ocean far to the west.

3. Low-order model

Without an active ocean dynamics, the above model is simple enough for us to focus on the ocean–atmospheric feedback through surface evaporation. A further simplification can be made by discretizing the model equations in the meridional direction. Such a low-order model has been derived in a zonally uniform case by Xie (1996a) using a staggered grid system shown in Fig. 5. The latitudinal asymmetry is represented by a single variable, the meridional wind velocity at the equator or, equivalently, the SST difference

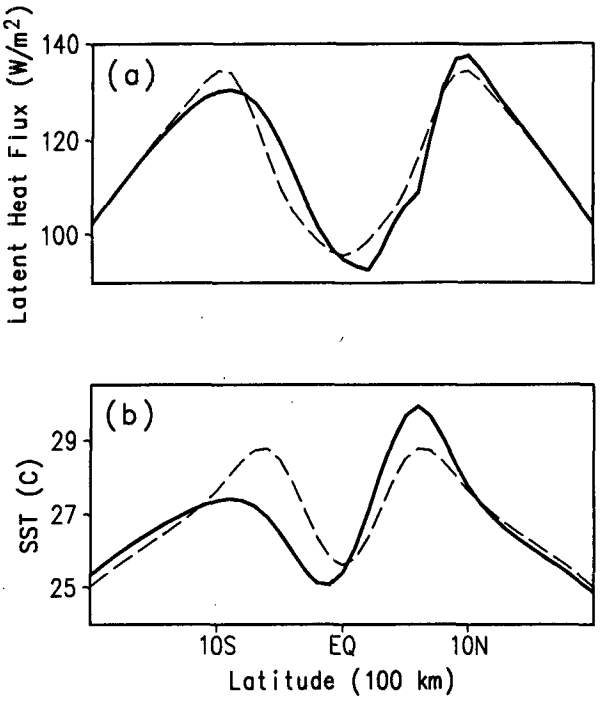

FIG. 4. Meridional distributions of (a) latent heat flux at the ocean surface and (b) SST at $x = -6400$ km for the symmetric (dashed line) and land-forced (solid) solutions.

between the two off-equatorial grids. This section applies the same scheme of meridional discretization and derives a zonally one-dimensional model that is mathematically tractable. A similar approach has been taken in deriving the so-called stripped down models of the ENSO that retain only latitudinally symmetric modes (Neelin 1991; Jin and Neelin 1993).

We take the symmetric solution such as the one shown in Fig. 1 as the basic state and denote it by an overbar. The low-order model considers only small deviations from the symmetric basic state. Hereafter, the notation is changed for clarity, with variables without an overbar denoting perturbation fields. For disturbances of large zonal scale and $\epsilon^2 \ll 1$, the longwave approximation applies, under which an equation for V can be derived from (2.1 ~ 3),

$$\frac{\partial^2 V}{\partial Y^2} + \left(\frac{1}{\epsilon}\frac{\partial}{\partial X} - Y^2\right)V = -\frac{\partial Q}{\partial Y} + \frac{Y}{\epsilon}\frac{\partial Q}{\partial X}. \quad (3.1)$$

An equation relating U to V is

$$\epsilon\frac{\partial U}{\partial Y} - Y\frac{\partial U}{\partial X} = V + Y\frac{\partial V}{\partial Y}. \quad (3.2)$$

Variables U and T share the same grid point (Fig. 5), which is placed off the equator at the latitude of hemispheric maximum of the basic state SST. Applying a center difference to the above equations at the equator leads to

$$V - X_0\frac{\partial V}{\partial X} = Y_P\hat{Q}, \quad (3.3)$$

$$\hat{U} = \frac{Y_P}{2\epsilon}V, \quad (3.4)$$

where $X_0 = Y_P^2/2\epsilon$ is the e-folding zonal scale of the atmospheric response to an antisymmetric heating, and the circumflex denotes the difference between the hemispheres; for example,

$$\hat{Q} = (Q_1 - Q_{-1})/2.$$

Note a notation change from (3.3) on, with V denoting the meridional wind speed at the equator. In deriving (3.3), boundary conditions,

$$V_1 = V_{-1} = 0, \quad (3.5)$$

have been used, which are approximately satisfied for equatorially antisymmetric disturbances as in the two-dimensional full model (Fig. 2).

For infinitesimal departures from the symmetric solution, the SST equation, (2.5), may be linearized as

$$\frac{\partial T}{\partial t} = aU - bT + \kappa\nabla^2 T, \quad (3.6)$$

where $a = (1/-\bar{U})(\bar{E}/c_p\rho h)$ and $b = (L/R^*\bar{T}^2)(\bar{E}/c_p\rho h)$ with $\bar{E} = -C_E^*\bar{U}q(\bar{T})$ being the evaporation rate. Only the effects of zonal wind deviation on the SST are considered since the mean meridional wind vanishes at the latitude of the ITCZ. At $Y = \pm Y_P/2$, where $\bar{T}$ is at its maximum and exceeds T_c, the heating function (2.4) may be linearized as

$$Q = \frac{K_Q}{(\beta C^3)^{1/2}}T.$$

Substituting it in (3.6) with the help of (3.4) yields an equation for the hemispheric difference in convective heating

$$\frac{\partial\hat{Q}}{\partial t} = \frac{\lambda}{2}Y_P V - b\hat{Q}, \quad (3.7)$$

where $\lambda = aK_Q/AC$. Note that the diffusion term has been absorbed into the Newtonian cooling term. By defining

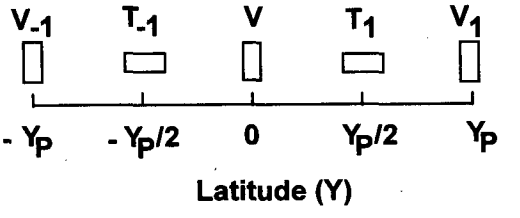

FIG. 5. Grid system for the low-order model.

$$\theta = Y_P \hat{Q}, \tag{3.8}$$

and rescaling time and space as

$$x^* = X/X_0, \tag{3.9a}$$

$$t^* = bt, \tag{3.9b}$$

we obtain from (3.3)

$$\left(1 - \frac{\partial}{\partial x^*}\right)V = \theta, \tag{3.10}$$

and from (3.7)

$$\left(\frac{\partial}{\partial t^*} + 1\right)\theta = \sigma V, \tag{3.11}$$

where

$$\sigma = \frac{\lambda Y_P^2}{2b} \tag{3.12}$$

is the nondimensional coupling coefficient (Xie 1996a). Equations (3.10) and (3.11) can be combined to form a single equation for V:

$$\left(\frac{\partial}{\partial t^*} + 1\right)\left(1 - \frac{\partial}{\partial x^*}\right)V = \sigma V. \tag{3.13}$$

The asterisk will be dropped hereafter for clarity. In the zonally symmetric case, the solution to (3.13) is a purely growing mode with a growth rate of $(\sigma - 1)$.

Under the longwave approximation, the characteristics of the atmospheric response to an equatorially asymmetric heat source are intrinsically different from those to a symmetric one. A symmetric heating affects the atmosphere both to the east and west by emitting Kelvin and Rossby waves. An antisymmetric heating, in contrast, excites only westward propagating Rossby waves, exerting no effect on the atmospheric circulation to the east [see Gill's (1980) Fig. 3]. Equation (3.10) is a discretized form of the Matsuno–Gill model, describing a forced, equatorially antisymmetric Rossby wave that propagates and decays toward the west. As conditions over the ocean ($x < 0$) do not affect the asymmetric circulation of the atmosphere to the east, it is therefore self-consistent to impose an eastern boundary condition,

$$V|_{x=0} = V_E, \tag{3.14}$$

where V_E denotes the latitudinally asymmetric atmospheric flow forced by one or a combination of the land effects listed in the preceding section. The following two sections obtain and analyze the steady-state and time-dependent solutions to (3.10) and (3.11) with the boundary condition (3.14).

4. Steady-state solution

Letting $\partial/\partial t = 0$, we obtain from (3.13)

$$\frac{dV}{dx} + (\sigma - 1)V = 0, \tag{4.1}$$

whose solution satisfying (3.14) is

$$V = V_E e^{-(\sigma-1)x}, \quad x < 0. \tag{4.2}$$

Whether or not the solution is symmetric is determined by the eastern boundary condition.[3] With nonzero latitudinal asymmetry at the eastern boundary, the asymmetry of the coupled ocean–atmosphere grows or decays toward the west, depending on the value of σ. This linkage of interior asymmetry to the growth rate of the WES instability will become clear in the next section, where the time dependent problem is solved. An interesting point to note is that even with a negative net growth rate $\sigma - 1 \lesssim 0$, the latitudinal asymmetry set by the eastern boundary condition can penetrate a great distance, in contrast to the zonally symmetric case, where the asymmetric solutions become impossible when the WES mode is stabilized. This is because the zonally varying case corresponds to a boundary-forced problem, whereas in the zonally symmetric case, latitudinal asymmetries arise only from the internal instability.

To see how the low-order model performs, we run the two-dimensional full model, imposing on the eastern boundary a wind velocity profile that is antisymmetric about the equator (Fig. 9a).[4] Figure 6 shows the meridional wind speed in logarithm as a function of longitude in the full 2D coupled model with several coupling coefficients. The exponential functional form predicted by the low-order model is well reproduced in the eastern two-thirds of the basin. The rapid decrease in the western basin is due to the decoupling effects of small wind speed in the basic state. With zero coupling,

[3] Using an anomaly coupling scheme, Xie (1994b) obtained an asymmetric solution to a 3D hybrid coupled OGCM under symmetric conditions. The basic state Xie (1994b) used is marked by cold SSTs below the threshold for convection ($T < T_c$) in the eastern ocean. As a result, the ITCZ gradually vanishes toward the east. As latitudinal asymmetries develop, the east end of the ITCZ extends eastward in one hemisphere and retreats westward in the other. Since the warm water band and the ITCZ do not reach the eastern boundary, the above linear solution under fixed boundary conditions does not apply.

[4] The wind profile is obtained by forcing the atmospheric model with a dipole, zonally uniform heating distribution confined to the east of the eastern boundary:

$$\frac{\sqrt{\beta C^3}}{K_Q^0} Q = \begin{cases} 0, & x \leq 0 \\ \Delta T_E(e^{-\frac{1}{2}[(y-y_0)/y_L]^2} - e^{-\frac{1}{2}[(y+y_0)/y_L]^2}), & x > 0. \end{cases} \tag{4.3}$$

The positive and negative poles are centered on $y = \pm y_0 = \pm 700$ km, with the scale of the Gaussian poles $y_L = 200$ km. A weak land heating $\Delta T_E = 0.1$°C is used. Figure 9a displays the wind field that the atmospheric model produces in response to this land heating.

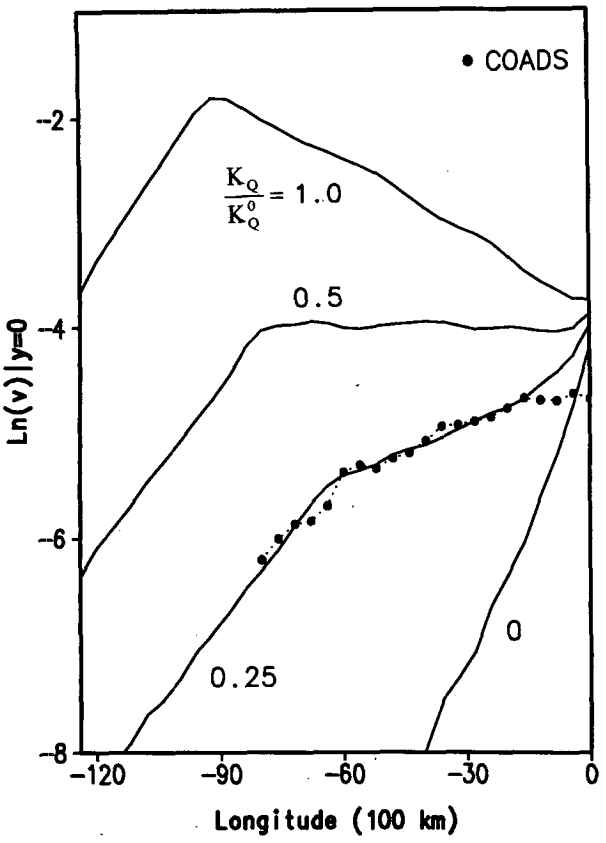

FIG. 6. Logarithm of meridional wind speed at the equator as a function of longitude. The COADS data are rescaled to fit the figure and shown in solid cycles.

the meridional wind is tightly trapped by the eastern boundary, with an e-folding scale of about 1000 km. As coupling intensifies, the latitudinal asymmetry penetrates deep into the interior ocean. At $K_Q = 0.5K_Q^0$, latitudinal asymmetry of the same magnitude is maintained throughout the central and eastern parts of the basin, resembling the $\sigma = 1$ solution to the low-order model with the linear WES mode at its neutral point. With stronger coupling, the latitudinal asymmetry of the model steady state amplifies westward, exceeding that on the eastern boundary.

The observed equatorial meridional wind speed based on the Comprehensive Ocean–Atmosphere Data Set (COADS) is also plotted in solid cycles in Fig. 6. The cross-equatorial wind reaches maximum on the west coast of the American continent and decreases westward. Its e-folding scale may be estimated to be 80° longitude or 9000 km, an order of magnitude greater than that of the decoupled curve. Clearly, latitudinally asymmetric ocean–atmosphere interactions such as the WES feedback are playing a crucial role in setting up the NH ITCZ across the Pacific basin. Taking one step further to a more quantitative discussion, one may be tempted to estimate the growth rate of the WES mode in the Pacific by measuring the slope of the observed curve. Such an estimation is too simplistic, however, as the zonal distribution of equatorial asymmetry is affected by nonlinearities (see section 6).

5. Time-dependent solutions

a. Plane waves

There exist plane wave solutions of the form

$$V \propto e^{i(kx-\omega t)} \tag{5.1}$$

to the low-order model equation (3.13). The dispersion relation is

$$i\omega = 1 - \frac{\sigma}{1 - ik}. \tag{5.2}$$

The growth rate of the wave mode is

$$\omega_i = \frac{\sigma}{1 + k^2} - 1, \tag{5.3}$$

which increases as the wavenumber decreases. The zonally symmetric mode has the largest growth rate, ensuring large zonal scales of latitudinally asymmetric features in the steady state. The frequency of the wave is given by

$$\omega_r = -\frac{\sigma k}{1 + k^2}, \tag{5.4}$$

which manifests a westward phase propagation. Interestingly, this westward propagating WES wave has a frequency–wavenumber relation exactly the same as that of a Rossby wave on a beta plane. This is purely accidental; the restoring force for a Rossby wave is the gradient of the potential vorticity in the basic state, whereas the restoring force for a WES wave is the feedback between the ocean and atmosphere as its frequency is proportional to the coupling coefficient σ. In the limit of $k \sim 0$, the WES waves are nondispersive. Unfortunately, however, this nondispersive limit is not applicable in the Pacific since $O(k) = 1$ if the basin size is used as the half-wavelength.

A schematic of the WES wave is shown in Fig. 7. The wave structures are antisymmetric about the equator. In response to an antisymmetric SST pattern with a positive perturbation to the north and a negative one to the south of the equator like the left half of the wave, the atmosphere produces southerly winds. Flowing across the equator to the Northern Hemisphere, the southerlies are turned eastward by the Coriolis force, inducing a westerly wind component. Similarly, zonal wind perturbations in the opposite direction are induced south of the equator. Superimposed on the prevalent easterly trade winds, the westerly perturbations reduce the wind speed and surface latent heat flux in the Northern Hemisphere, whereas the easterly perturbations enhance them in the Southern Hemisphere. The

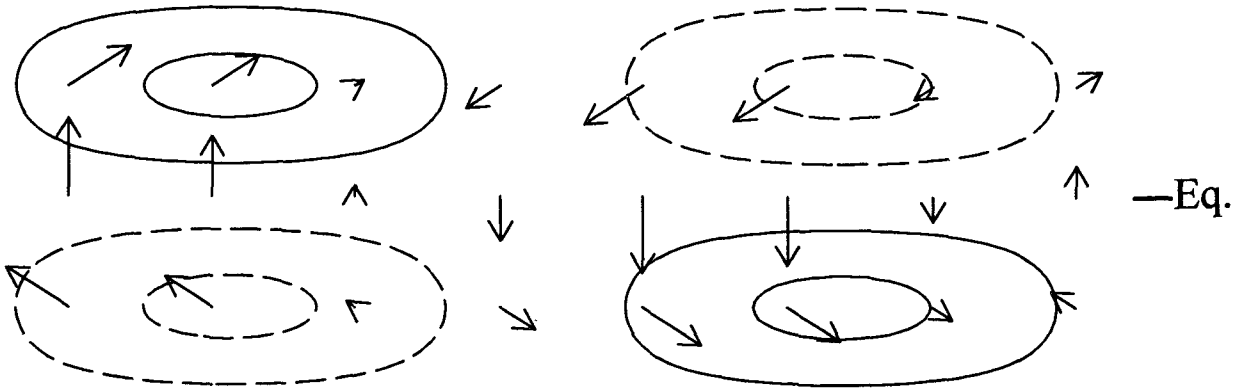

FIG. 7. Schematic of the westward propagating WES instability. Contours are for SST and vectors for surface wind velocity.

antisymmetric perturbations in the latent heat flux thus amplify the initial SST perturbations, closing a positive feedback loop of wind → evaporation → SST. In the presence of zonal variation, atmospheric Rossby waves carry wind perturbations westward away from where they are forced, causing the coupled instability to propagate westward. The westward phase shift of the wind perturbation can be seen in Fig. 7.

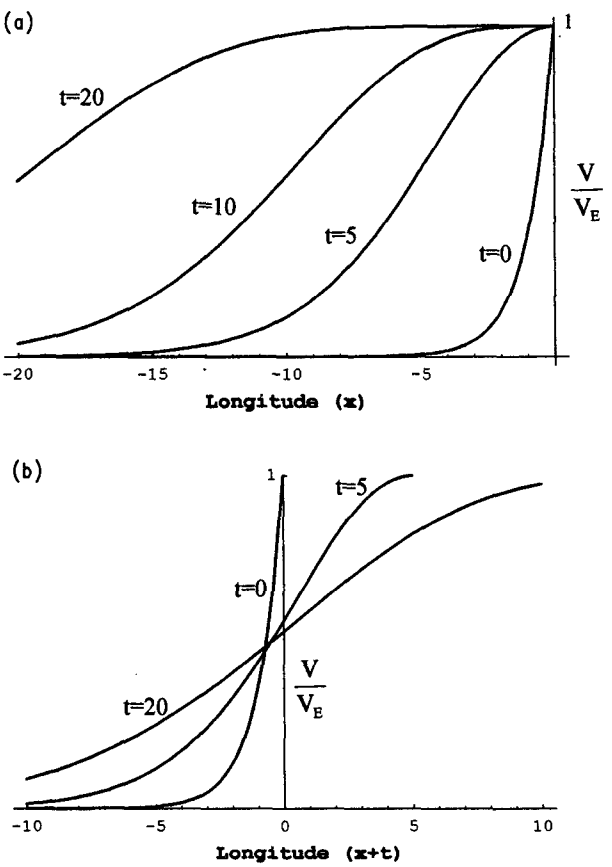

FIG. 8. Time evolution of meridional wind velocity at the equator as a function of longitude in the zonally one-dimensional model: (a) in physical space and (b) in a coordinate moving westward at the phase speed of the long WES wave.

b. *Initial value problem*

This subsection solves initial value problems and examines how a latitudinally asymmetric steady state is established from a symmetric initial condition. This serves to illustrate the roles of the westward propagating WES mode. Consider an initial state that corresponds to the uncoupled case of $K_Q = 0$. By setting $\sigma = 0$, the solution to (3.13) satisfying the boundary condition (3.14) is

$$V|_{t=0} = V_E e^x, \tag{5.5}$$

which has a coastally trapped structure. The corresponding initial temperature field is

$$\theta|_{t=0} = 0. \tag{5.6}$$

We then switch on the oceanic feedback and let the coupled system to evolve. The solution to the combined initial boundary value problem of (3.13), (3.14), and (5.5) is

$$V = V_E e^{-(\sigma-1)x} \times \left[1 - \frac{e^{-t}}{2}\int_0^{2\sqrt{-\sigma x}} \xi e^{-(\xi^2/4)} \mathrm{I}_0(\xi\sqrt{t})\, d\xi\right], \tag{5.7}$$

where I_0 is the modified Bessel function of order 0 (see appendix).

Figure 8 displays the time-dependent solution for $\sigma = 1$, with which the zonally symmetric WES mode is neutral. Upon the switch-on of the oceanic feedback, a wave front moves westward off the eastern boundary, building up latitudinal asymmetry on the way (Fig. 8a). The WES waves are the transmitter that sends westward the signal of latitudinal asymmetry imposed on the boundary. After the passage of the WES wave front, an asymmetric steady state is established. The

front of WES waves broadens with time, as can be seen in a coordinate moving westward at the phase speed of the longwave, $c = \sigma = 1$ (Fig. 8b). For arbitrary values of σ, the properties of wave propagation remain the same except that the x coordinate is compressed by a factor of σ [see (5.7)]. The wave front amplifies for $\sigma > 1$ but decays for $\sigma < 1$ as it moves westward. The wave front is neutral with a constant amplitude for $\sigma = 1$. Since the WES wave front is the agent that sets up the latitudinal asymmetry, its stability determines the functional form of the steady-state solution (4.2).

The same type of initial value problem is solved with the two-dimensional full model for $K_Q = K_Q^0$ and $\Delta T_E = 1$°C. Figure 9 shows the time evolution of the solution. With zero SST anomalies at $t = 0$, land forcing-induced asymmetric winds are trapped near the eastern boundary, characterized by westerly and easterly anomalies in the Northern and Southern Hemisphere, respectively (Fig. 9a). Upon the switch-on of the oceanic feedback, this wind anomaly pattern, through latent heat flux, induces a SST anomaly pattern with positive (negative) sign in the Northern (Southern) Hemisphere (Fig. 9b). This SST anomaly pattern excites additional long Rossby waves in the atmosphere, expanding the west edge of the wind anomaly pattern. As a result, the whole coupled ocean–atmospheric anomaly pattern moves westward. The model reached a steady state in five years. The transient ocean–atmospheric anomaly patterns resemble those of the one-dimensional WES waves shown in Fig. 7, suggesting that the westward propagation mechanism is essentially the same in these two models. The simple low-order model thus serves as a useful tool for illustrating the basic characteristics of both the transient and steady-state response to land forcing. Because of the coarse meridional resolution of the low-order model, quantitative comparison with the two-dimensional model is not appropriate. The low-order model should be used for qualitative discussion only.

Latent heat flux is normally treated as one forcing term in the SST equation without discriminating contributions between wind speed and SST variations. As

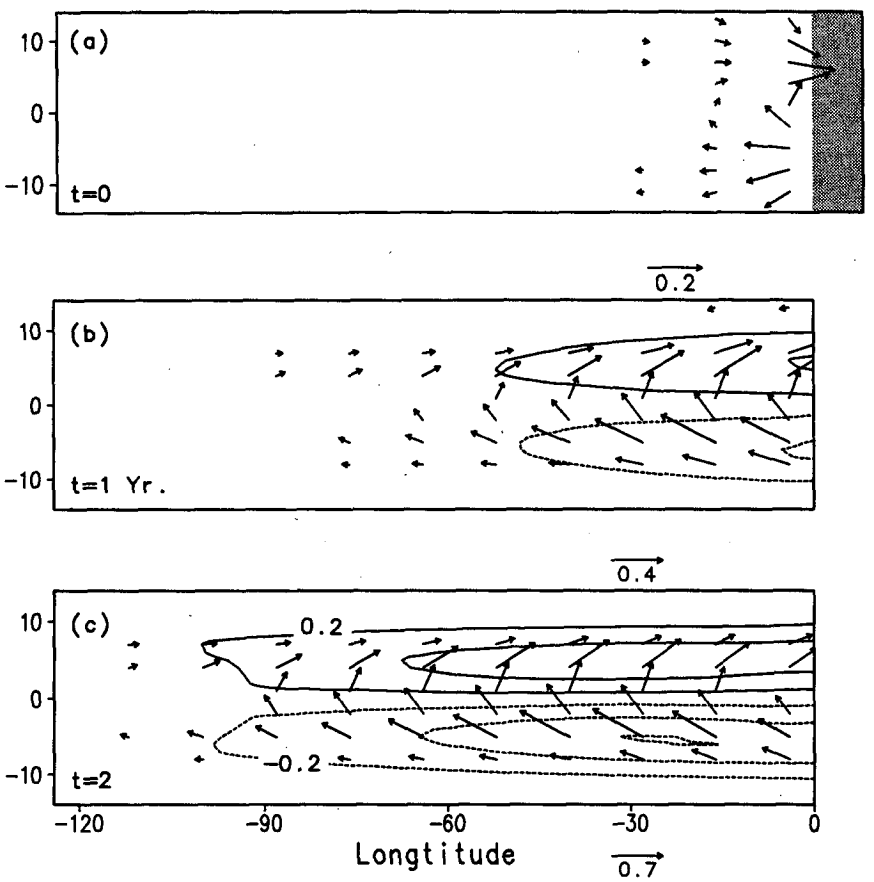

FIG. 9. Transient response of the coupled model to an equatorially antisymmetric heating distribution over land [(4.3) with $\Delta T_E = 1$°C; land surface shaded]. Contours are for SST anomalies with intervals of 0.4°C and vectors for wind velocity with the scale shown beneath each panel. At $t = 0$ SST anomalies are zero.

seen in Fig. 4, large SST changes can occur without significant changes in latent heat flux due to the canceling effect of wind speed. Figure 10 shows how latent heat flux, wind speed, and SST adjust in the transient problem. At 8°S, the WES waves from the east intensify the trade winds and lower SST. Initially, the increasing winds dominate the change in latent heat flux, causing it to increase. The resultant decrease in SST acts to halt the increase in latent heat flux, which peaks after two years. The SST effect then takes over and latent heat flux is relaxed back to its initial value despite the continuous increase in wind speed. During the adjustment, extra latent heat is released from the ocean, consistent with the SST decrease. Comparing latent heat flux in the steady states before and after the adjustment does not help explain the cause of the SST change, unless the latent heat flux is decomposed into wind and SST contributions as in (3.6).

The WES waves seem to exist in some state-of-the-art coupled GCMs. Upon applying a localized forcing near the east end of the Pacific, disturbances are observed in these GCMs, carrying latitudinal asymmetric signals westward across the basin (C. Ma and C. Mechoso 1995, personal communication; M. Kimoto and X. Shen 1995, personal communication). Heat budget analysis reveals that the wind-speed-induced changes in latent heat flux is the major cause for establishing latitudinal asymmetry of SST in the GCM's transient adjustment.

6. Nonlinear effects

We now return to the steady-state problem. Being a useful tool for understanding the full model, the linear low-order model is not valid for large boundary forcing as nonlinearity becomes important. Figure 11a shows

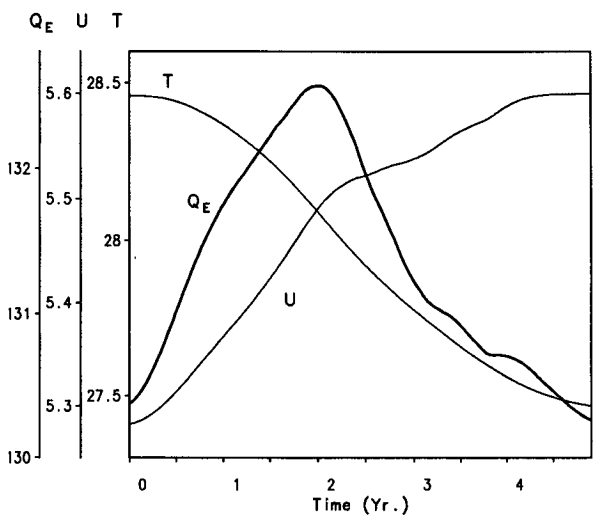

FIG. 10. SST (°C), wind speed (m s^{-1}), and latent heat flux (W m^{-2}) at $x = -6400$ and $y = -800$ km as functions of time.

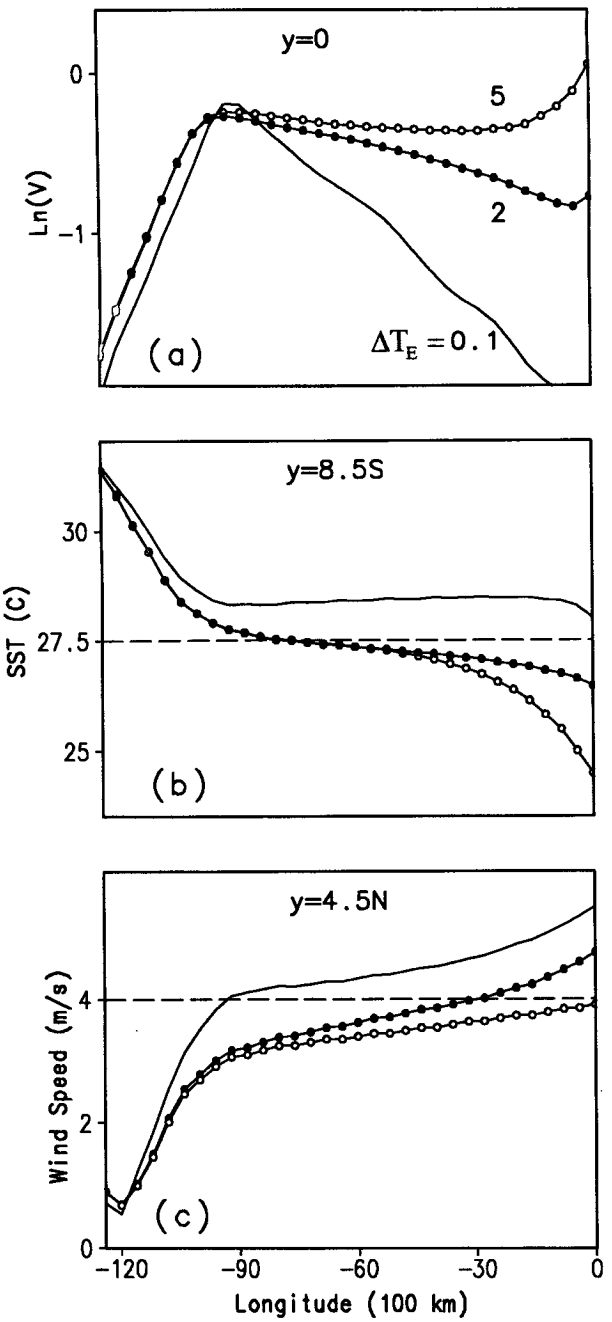

FIG. 11. Solutions for different land forcing amplitudes: (a) logarithm of meridional wind velocity at the equator [ln(5V) for ΔT_E = 0.1°C], (b) SST at 8.5°S, and (c) scalar wind speed at 4.5°N.

the logarithm of the meridional wind speed along the equator for different boundary forcing amplitudes. The low-order model fares well for small boundary forcing with $\Delta T_E = 0.1$°C, predicting that the meridional wind amplifies westward exponentially at a constant rate proportional to the growth rate of the WES instability. As the boundary forcing increases, the development of lat-

itudinal asymmetry lowers the SST in the Southern Hemisphere and pushes it below the threshold for convection (Fig. 11b). As a result, the atmosphere and ocean are decoupled in the Southern Hemisphere, reducing the growth rate of the WES instability. This is manifested by a significant reduction in the slope of the curve for $\Delta T_E = 2.0$°C in Fig. 11a. Another important nonlinearity is the minimum wind requirement for scalar wind speed in surface evaporation calculation. Further increase in the boundary forcing weakens the NH trades so much that the wind speeds are below the minimum wind threshold (the $\Delta T_E = 5.0$°C curve in Fig. 11c). This decouples the ocean from the atmosphere in the Northern Hemisphere, leading to a further reduction in the slope of the meridional wind in Fig. 11a. In summary, the nonlinearities reduce the growth rate of the WES instability by shutting off the coupling between the ocean and atmosphere.

The eastern Pacific obviously falls in the nonlinear regime; deep convection in the Southern Hemisphere is suppressed and the winds in the NH ITCZ are very weak. This makes it difficult to estimate the linear WES growth rate from the observations. The slope of the annual mean meridional wind speed at the equator does not equal the linear WES growth rate itself, but is a fingerprint of the WES mode that evolves through nonlinear stages. Despite these difficulties, the slow westward decrease of latitudinal asymmetry revealed by the COADS seems to suggest that the linear growth rate of the Pacific should not be too far from the neutral point, probably being either marginally stable or marginally unstable.

7. Discussion

The problem of latitudinal asymmetry of the tropical climatology is investigated using a coupled ocean–atmosphere model. Equatorially antisymmetric wave modes are found to exist in the coupled system, which grows with time and propagates westward by a wind–evaporation–SST feedback mechanism. A linear low-order version of the model that retains only the antisymmetric modes is found to be useful for understanding the growth and the phase propagation of coupled disturbances. The destabilizing mechanism of the WES modes is the same as in the zonally symmetric model of Xie (1996a). In the presence of zonal variations, wind perturbations in the form of atmospheric Rossby waves are located to the west of SST perturbations, causing the phase of the coupled instability to move westward. Interestingly, the WES wave has the same frequency–wavenumber relation as the beta-plane Rossby wave, although the coincidence is purely accidental. The growth rate of the WES wave is an increasing function of wavelength, ensuring that latitudinally asymmetric features emerging from the model have large zonal scales.

Hemispheric asymmetries of continental geometry have long been suspected to be the cause of the observed latitudinal asymmetry of tropical Pacific climatology. A transmitter, necessary to inform the interior ocean far away of these geographic asymmetries on continents, has been missing. This paper proposes the westward propagating WES wave as the missing transmitter. Here the symmetry breaking effects of land geography are treated implicitly and imposed as the eastern boundary condition. Without the oceanic feedback, the influence of the land forcing is tightly trapped by the eastern boundary in the form of damped atmospheric Rossby waves. When the oceanic feedback is activated, the WES waves become the eigenmodes of the coupled system. In an initial value problem, the latitudinal asymmetry generated by the boundary condition moves off the eastern boundary and penetrates deep into the west in the form of a WES wave front, much like the spinup of the subtropical gyre in response to a sudden switch-on of wind curls as shown by Anderson and Gill (1975). Depending on the growth rate of the WES instability, the wave front amplifies or decays as it moves westward, leaving behind a latitudinally asymmetric climate. The coupled model predicts an exponential distribution of latitudinal asymmetry in the zonal direction, consistent with observations in the eastern Pacific, where the logarithm of the COADS annual-mean meridional wind speed appears to be a linear function of longitude along the equator.

In a zonally uniform setting as on a water-covered planet, a positive WES growth rate is required to break the equatorial symmetry set by the annual mean solar radiation. In order to reach a steady state on such an aquaplanet, the growth by the WES feedback has to be suppressed by such nonlinearities as the SST threshold for atmospheric deep convection and/or the minimum wind speed requirement for calculating evaporation, which shut off the coupling between the ocean and atmosphere. In contrast to the nonlinear nature of the steady-state problem on an aquaplanet, the problem is essentially linear when zonal variations are allowed and latitudinally asymmetry is set up somewhere externally by land geography. The latitudinal asymmetry is established by the passage of the WES wave front emitted from the eastern boundary. The linear WES growth rate affects only zonal distribution of latitudinal asymmetry in the land-forced problem. Even with a negative growth rate, the WES mode can penetrate a great distance to the west, carrying latitudinal asymmetry with it. The above difference between the zonally symmetric and asymmetric cases arises because the former is a free mode problem, whereas the latter is a boundary forced problem.

The basic state of the ocean, assumed to be zonally uniform in this paper, varies greatly over the Pacific. The changes in the mixed layer depth gives rise to spatial variations in both the coupling coefficient σ and the damping rate b. For a zonally varying basic state, the steady-state solution to the low-order model equations (3.10) and (3.11) is

$$V = V_E \exp\left[-\int_0^x (\sigma - 1)dx\right]. \quad (7.1)$$

Here, the coupling coefficient σ may include not only the WES but other feedbacks as well. A feedback that displays large zonal variations in the eastern Pacific is the one associated with clouds. Off the west coast of South America, a positive feedback is at work between low-level stratiform clouds and local SST, with stratus clouds that form over cold ocean surface shielding solar radiation. Philander et al. (1996) show that the inclusion of this stratus-SST feedback leads to enhanced latitudinal asymmetry in a coupled GCM. West of 90°W, on the other hand, cloud forcing is dominated by that associated with deep cumulus clouds to the north of the equator as seen in the cloud albedo distribution (e.g., Fig. 9b of Mitchell and Wallace 1992). The feedback becomes negative between cumulus clouds and SST, with cumuli over high SSTs cooling the ocean surface. Although narrow, with a zonal extent of 10° longitude, the stratus cloud zone off South America could act as an amplifier in passing westward the latitudinal asymmetry forced by land geometry. West of the stratus cloud zone, other ocean–atmosphere interaction mechanisms, such as the WES feedback, are necessary to overcome the negative cumulus–SST feedback and sustain the NH ITCZ.

The absence of a perennial NH ITCZ in the Indian and western Pacific Oceans seems to be attributable to their annual mean wind fields. In an environment of westerly mean wind as in the Indian Ocean, the WES feedback is negative, bringing back any departures from the equatorial symmetry. The small annual-mean wind speeds in these two oceanic sectors make the annual-mean winds irrelevant to evaporation, which is instead controlled by such atmospheric disturbances as westerly bursts and intraseasonal oscillations. The situation in the Atlantic seems rather simple, with the bulge of the African continent being the primary cause of the NH ITCZ. While both have larger land mass to the north of the equator, the Indian and Atlantic Oceans have very different climatologies in terms of their latitudinal asymmetry because of the differences in the direction and the magnitude of the prevalent winds. In the Pacific, ocean–atmosphere interaction is responsible for establishing the NH ITCZ, with land geographic asymmetries providing seeds favorable for the Northern Hemisphere. Many geographic features of the American continents, some of which are listed in section 2, may contribute to the latitudinal asymmetry of the Pacific climatology. Their individual roles and collective effects need to be investigated.

Acknowledgments. The author would like to thank Atsushi Kubokawa for suggesting the Laplace transformation method, Taroh Matsuno for a helpful discussion on seasonal forcing, Tim Li and George Philander for preprints, and anonymous referees for comments helpful in improving the presentation of results. Some of the figures are produced with the GrADS developed by Brian Doty. This work was supported by grants from the Japanese Ministry of Education, Culture and Science and from the Center for the Climate System Research of the University of Tokyo. Preliminary results from a hybrid coupled OGCM that eventually led to this study were presented at a seminar at GFDL in 1992, while the author was a visiting scientist at Princeton University.

APPENDIX

Solution to the Initial Value Problem

Applying the Laplace transformation to (3.13) with respect to $-x$ with the help of the formula

$$\frac{1}{p} e^{-(1/p)} \underset{\text{Inverse}}{\overset{\text{Laplace}}{\leftrightarrows}} I_0(2\sqrt{z})$$

leads to (5.7). Since $I_0(z)$ is a monotonical increasing function, an upper bound for the integral in (5.7) can be obtained:

$$\int_0^{2\sqrt{-\sigma x}} \xi e^{-(\xi^2/4)} I_0(\xi\sqrt{t}) d\xi \leq 4(-\sigma x) e^{\sigma x} I_0(2\sqrt{-\sigma x t}). \quad (A.1)$$

An asymptotic form of the above upper bound for large t is

$$\int_0^{2\sqrt{-\sigma x}} \xi e^{-(\xi^2/4)} I_0(\xi\sqrt{t}) d\xi \leq 2\left[\frac{(-\sigma x)^3}{\pi^2 t}\right]^{1/4} e^{\sigma x} e^{2\sqrt{-\sigma x t}}, \quad (A.2)$$

where

$$I_v(z) \approx (2\pi z)^{-1/2} e^z, \quad \text{for large } z$$

is used. The time dependence of the rhs of (A.2) is $e^{2\sqrt{-\sigma x t}}/t^{1/4}$, whose growth is much slower than the decay of the term e^{-t} for large t. The second term in the bracket of the rhs of (5.7) thus decays exponentially with time at the rate of the oceanic Newtonian cooling. As time goes to infinity, the time-dependent solution (5.7) approaches the steady-state solution (4.2).

REFERENCES

Anderson, D. L. T., and A. E. Gill, 1975: Spin-up of a stratified ocean, with applications to upwelling. *Deep-Sea Res.*, **22,** 583–596.

——, and J. P. McCreary, 1985: Slowly propagating disturbances in a coupled ocean–atmosphere model. *J. Atmos. Sci.*, **42,** 615–629.

Gill, A. E., 1980: Some simple solutions for heat-induced tropical circulation. *Quart. J. Roy. Meteor. Soc.*, **106,** 447–462.

Hess, P. G., D. S. Battisti, and P. J. Rasch, 1993: The maintenance of the intertropical convergence zones and the large-scale tropical circulation on a water-covered earth. *J. Atmos. Sci.*, **50,** 691–713.

Hirst, A. C., 1986: Unstable and damped equatorial modes in simple coupled ocean–atmosphere models. *J. Atmos. Sci.*, **43,** 830–852.

Jin, F.-F., and J. D. Neelin, 1993: Modes of interannual tropical ocean–atmosphere interaction—A unified view. Part I: Numerical results. *J. Atmos. Sci.*, **50,** 3477–3503.

Kornfield, J., A. F. Hasler, K. J. Hanson, and V. E. Suomi, 1967: Photographic cloud climatology from ESSA III and V computer produced mosaics. *Bull. Amer. Meteor. Soc.*, **48,** 878–882.

Li, T., and S. G. H. Philander, 1996: On the annual cycle of the eastern equatorial Pacific, *J. Climate,* **9,** (12, Part I), in press.

Manabe, S., D. G. Hahn, and J. L. Holloway, 1974: The seasonal variation of the tropical circulation as simulated by a global model of the atmosphere. *J. Atmos. Sci.*, **31,** 43–83.

Matsuno, T., 1966: Quasi-geostrophic motions in the equatorial area. *J. Meteor. Soc. Japan,* **44,** 25–43.

Mechoso, C. R., and Coauthors, 1995: The seasonal cycle over the tropical Pacific in general circulation models. *Mon. Wea. Rev.*, **123,** 2825–2838.

Mitchell, T. P., and J. M. Wallace, 1992: The annual cycle in equatorial convection and sea surface temperature. *J. Climate,* **5,** 1140–1156.

Neelin, J. D., 1991: The slow sea surface temperature mode and the fast-wave limit: Analytical theory for tropical interannual oscillations and experiments in a hybrid coupled model. *J. Atmos. Sci.*, **48,** 584–606.

——, and F.-F. Jin, 1993: Modes of interannual tropical ocean–atmosphere interaction—A unified view. Part II: Nonlinear cases. *J. Atmos. Sci.*, **50,** 3504–3522.

——, and H. A. Dijkstra, 1995: Ocean–atmosphere interaction and the tropical climatology. Part I: The dangers of flux correction. *J. Climate,* **8,** 1325–1342.

——, F.-F. Jin, and M. Latif, 1994: Dynamics of coupled ocean–atmosphere models: The tropical problem. *Annu. Rev. Fluid Mech.*, **26,** 617–659.

Numaguti, A., and Y.-Y. Hayashi, 1991: Behavior of cumulus activity and the structures of circulations in an "aqua-planet" model. Part II: Eastward-moving planetary scale structure and the Intertropical Convergence Zone. *J. Meteor. Soc. Japan,* **69,** 563–579.

Philander, S. G. H., D. Gu, D. Halpern, G. Lambert, N.-C. Lau, T. Li, and R. C. Pacanowski, 1996: Why the ITCZ is mostly north of the equator. *J. Climate,* **9,** (12, Part I), in press.

Robertson, A. W., C.-C. Ma, C. R. Mechoso, and M. Ghil, 1995: Simulation of the tropical Pacific climate with a coupled ocean–atmosphere general circulation model. Part I: The seasonal cycle. *J. Climate,* **8,** 1178–1198.

Xie, S. P., 1994a: Oceanic response to the wind forcing associated with the intertropical convergence zone in the Northern Hemisphere. *J. Geophys. Res.*, **99,** 20 393–20 402.

——, 1994b: The maintenance of an equatorially asymmetric state in a hybrid coupled GCM. *J. Atmos. Sci.*, **51,** 2602–2612.

——, 1996a: Unstable transition of the tropical climate to an equatorially asymmetric state in a coupled ocean–atmosphere model. *Mon. Wea. Rev.*, **9,** 2945–2950.

——, 1996b: Effects of seasonal solar forcing on latitudinal asymmetry of the ITCZ. *J. Climate,* in press.

——, and S. G. H. Philander, 1994: A coupled ocean–atmosphere model of relevance to the ITCZ in the eastern Pacific. *Tellus,* **46A,** 340–350.

——, A. Kubokawa, and K. Hanawa, 1989: Oscillations with two feedback processes in a coupled ocean–atmosphere model. *J. Climate,* **2,** 946–964.